

Magnetohydrodynamic Pumps with Permanent Magnets for Pumping Molten Metals or Salts

Ivo Dolezel¹, Vaclav Kotlan², Bohus Ulrych², and Vaclav Valenta³

¹Czech Technical University, Faculty of Electrical Engineering, Praha, Czech Republic

²University of West Bohemia, Faculty of Electrical Engineering, Plzen, Czech Republic

³ŠKODA JS a. s. (Nuclear Machinery), Plzen, Czech Republic

E-mail: dolezel@fel.cvut.cz, vkotlan@kte.zcu.cz, ulrych@kte.zcu.cz

Abstract:

Possibilities of pumping molten metals and salts (as cooling agents in nuclear reactors) by magnetohydrodynamic (MHD) pumps with permanent magnets are investigated. The principal attention is paid to the steady-state movement of these coolants in the closed cooling loops described by the balance of the Lorentz force produced by the pump and hydrodynamic drag forces. The methodology is illustrated on two typical examples whose results are discussed.

INTRODUCTION

High temperature nuclear reactors and modern “operator-free” mini-reactors use for transfer of thermal energy from the active area either molten metals (Na, Pb) and their alloys (Pb-Bi) or molten salts (especially fluoride salts). But pumping of these media by means of classical mechanical pumps is problematic. The technical realization of such pumps (mostly radial or axial pumps with rotors rotating in molten metals or salts) is very difficult and their lifetime is (due to the presence of movable parts and extremely unfavorable operation conditions) rather low.

It is clear that more promising and more reliable would be pumps without moving parts, making use of the force effects of electromagnetic fields. The first studies on these pumps can be found already at the end of the 1950s (e.g., [1] and [2]). Since then, the development in the domain has been very fast and to the date several different conceptions have been proposed. From the constructional viewpoint the simplest and very prospective seem to be MHD pumps with magnetic field generated either by a system of suitably shaped (saddle) coils carrying direct current or, in smaller applications, by appropriately arranged permanent magnets.

But mainly in the last case it is necessary to solve several additional serious problems. As known, the magnetic flux density of currently existing magnetic circuits with permanent magnets is limited by a value of about 2 T. It is not too much, particularly when the pumps work in nonstandard operation regimes (we can mention, for instance, transient phenomena – e.g., at the start after a prolonged shutdown of the mini-reactor – requiring relatively high pumping force that has to overcome various hydrostatic and hydrodynamic drag forces). The pumping force is achieved by interaction of the current density and magnetic flux density in the transported medium (see chapter 3, equation 7). And this can be a problem, mainly if the cooling agent is molten salt whose

electrical conductivity (Tab. 1) is typically by several orders of magnitude lower than, for example, conductivity of molten sodium. Optimization of the magnetic circuit for the purpose of obtaining the highest possible and sufficiently uniform magnetic flux density in the working channel, therefore, is a must.

Tab. 1: The basic physical parameters of considered heat-transfer media of the cooling loop

			sodium	fluoride salt (*)
working temperature (**)	T_{work}	[°C]	455	690
specific mass	ρ	[kg/m ³]	827.3	1972
electric conductivity	γ_{el}	[S/m]	4.757×10^6	501.3
thermal conductivity	λ	[W/(m K)]		0.9194
specific heat	c_p	[J/(kg K)]	1200	1850
kinematic viscosity	ν	[m ² /s]	2.734×10^{-7}	1.255×10^{-6}

(*) Fluoride salt LiF-NaF-KF (45.3-13.2-41.5 [mol%])

(**) Average value

The paper solves the above problems on a high temperature operator-free mini-reactor RAPID cooled with molten sodium as well as molten fluoride salt FLiNaK (LiF-NaF-KF (45.3-13.2-41.5 mol %)). This reactor of thermal output 10 MW and electrical output 1 MW was designed in the Central Research Institute of Electric Power Industry (CRIEPI), Japan [3] and its scheme is depicted in Fig. 1. In case of the fluoride salts we will not deal with the problems of their impact on the nuclear situation of the considered reactor, but only with their influence on the heat transfer and overall hydrodynamic conditions in the cooling loops.

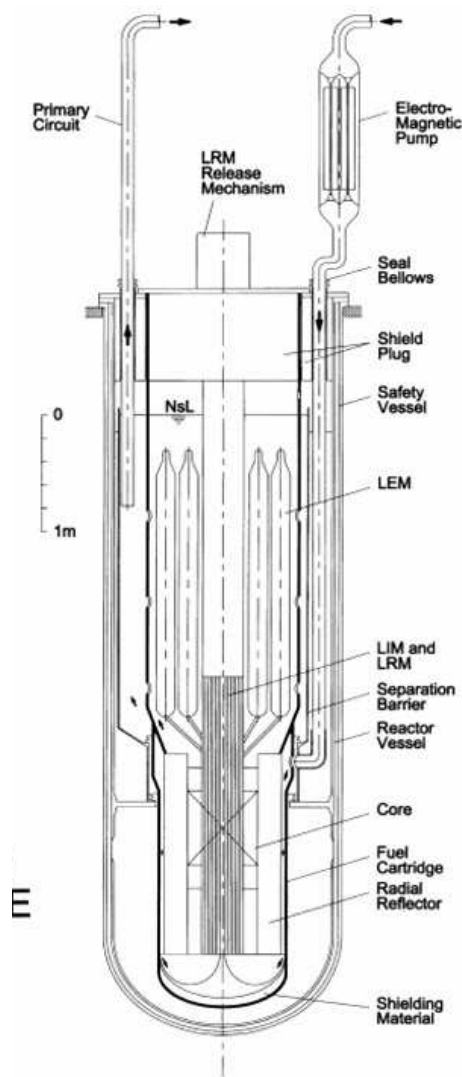


Fig. 1: Scheme of the high-temperature mini-reactor RAPID 1 MW E (taken from [1])

FORMULATION OF THE PROBLEM

Principle of operation of the MHD pump

The principle of the MHD effect-based pumping of electrically conductive non-ferromagnetic fluids (molten metals or salts) is explained in Fig. 2. Direct current I_e passes in the transversal direction of the working channel with heat-transfer medium **1** between two nonferromagnetic (and heatproof) electrodes **E1** and **E2**. The vector of the corresponding current density $J_e(x, y)$ is mostly oriented in parallel with the x -axis, thus perpendicularly to the longitudinal axis z of the channel. Magnetic field $B_m(x, y)$ (see Fig. 2) produced by appropriately formed saddle coils or a system of permanent magnets is supposed to be oriented almost perpendicularly to both the axis of the channel and vector $J_e(x, y)$. The interaction of both above vectors produces the Lorentz force (its vector

F_L being oriented in the direction of the z -axis) that pushes the molten metal upwards.

Basic parameters of the considered cooling loop

The cooling loop under investigation is depicted in Fig. 3. Its basic components and physical parameters are summarized in Tab. 2.

In order to obtain its parameters it was necessary to compute the hydrodynamic losses in their individual parts. The results serving for the first indicative dimensioning of the MHD pump are summarized in Tab. 3. The calculations were carried out on the basis of theoretical and empirical relationships (taken from [4], [5] and [6]) commonly used for solution of the hydrodynamic problems.

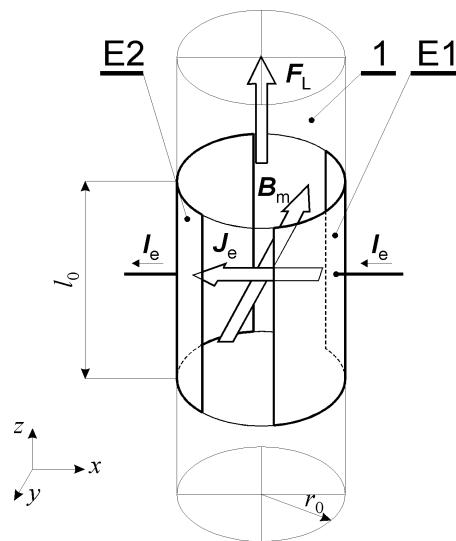


Fig. 2: Principal scheme of the pump: **1** – column with the working medium, **E1**, **E2** – electrodes

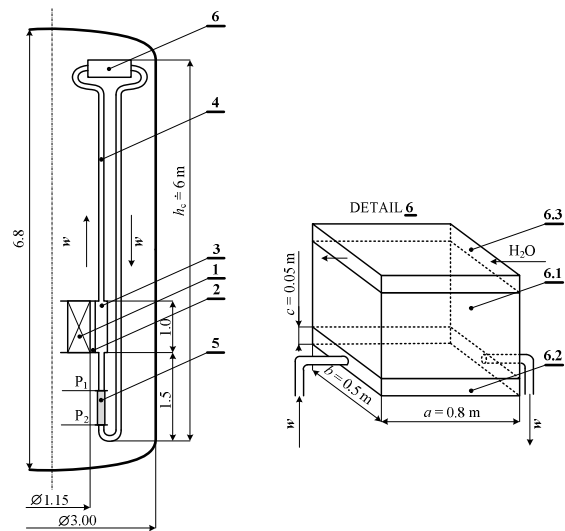


Fig. 3: Cooling loop arrangement: **1** active reactor zone; **2** shielding shell ($U_{238} \rightarrow Pu$); **3** cooling shell – heat exchanger; **4** cooling loop pipeline; **5** MHD pump in cooling shell (H_2O); **6** thermoelectric generator; **6.1** thermocouples block; **6.2** "hot" chamber (sodium or fluoride salt FLiNaK); **6.3** "cold" chamber (cooling water)

Tab. 2: Basic structural and physical parameters of the considered cooling loop

			working medium	
			sodium	fluoride salt
thermal output of the reactor	P_{th}	[MW]	10	
maximal temperature of the working medium	T_{max}	[°C]	530	775
minimal temperature of the working medium	T_{min}	[°C]	380	625
mass flow rate of coolant	G_{cool}	[kg/s]	52.5	36.04
volume flow rate of coolant	V_{cool}	[m ³ /s]	0.06217	0.01828
cooling shell of the reactor (carrying the working liquid)	D_{min}	[mm]	1400	
	D_{max}	[mm]	1500	
diameter of the pipe of the cooling loop	$D_0 = 2r_0$	[mm]	130	75
velocity of flow in the cooling loop	w_s	[m/s]	1	
hydrostatic pressure in the cooling loop	Δp_{hs}	[Pa]	4.869×10^4	1.611×10^5
hydrodynamic pressure (*) in the cooling loop	Δp_{hd}	[Pa]	5.277×10^2	$7.140 \cdot 10^2$
hydrostatic drag force in the cooling loop	F_{hs}	[N]	646.3	711.7
hydrodynamic drag force in the cooling loop	F_{hd}	[N]	7.001	3.154
total pumping force (**) in the cooling loop	F_L	[N]	10.50	4.731

(*) for more details see Tab. 3

(**) generated by an MH pump with the coefficient of safety $\kappa_b = 1.5$

Tab. 3: Hydrodynamic losses in particular elements of the considered cooling loop

			working medium	
			sodium	fluoride salt
hot branch of the loop	Δp_{p1}	[Pa]	232.	219.3
hot knee ($R_0 = 0.4$ m, $\delta = 90^\circ$)	Δp_{p2}		1.575	5.782
hot knee ($R_0 = 0.4$ m, $\delta = 180^\circ$)	Δp_{p3}		3.148	11.56
cooling shell of the reactor	Δp_{p4}		0.07111	0.6823
hot chamber of the thermoelectric generator	Δp_{p5}		0.491	6.106
cold branch of the loop	Δp_{p6}		284.6	239.2 (*)
cold knee ($R_0 = 0.4$ m, $\delta = 90^\circ$)	Δp_{p7}		1.008	5.782 (*)
two cold knees ($R_0 = 0.4$ m, $\delta = 180^\circ$)	$2 \times \Delta p_{p8}$		2×2.016	2×11.56 (*)
Σ			527.7	714.0

(*) the dependence of viscosity on temperature is not known

Tab. 4: Basic physical properties of materials of the considered pump

item (*)	pump element	material	characteristic values
<u>1</u>	transported working medium	molten sodium molten fluoride salt	see Tab. 1
<u>2</u>	electrodes	austenitic steel ČSN 17 030	$\gamma_{el} = 1.5 \times 10^6$ [S/m] $\mu_r = 1$ [-]
<u>3</u>	channel	molten basalt	$\gamma_{el} = 1 \times 10^{-6}$ [S/m] $\mu_r = 1$ [-] $\lambda = 2$ [W/(mK)]
<u>4</u>	ferromagnetic focusators	carbon steel ČSN 12 040	μ_r see Fig. 6 λ see Fig. 7
<u>5</u>	magnets heat insulation	fiberglass	$\gamma_{el} = 1 \times 10^{-6}$ [S/m] $\mu_r = 1$ [-] $\lambda = 0.04$ [W/(mK)]
<u>6</u>	ferromagnetic bypasses	carbon steel ČSN 12 040	μ_r see Fig. 6 λ see Fig. 7

7	permanent magnets	NdFeB Magnet, Grade GSN-40 [5]	$H_c = 9.555 \times 10^5$ [A/m]
			$B_r = 1.27$ [T]
			$T_w = 150$ [°C]
			$\mu_r = 1.0577$ [-]
8	cooling water	H ₂ O	$\mu_r = 1$ [-]
			$T_0 = 20$ [°C]

(*) see Fig. 4

Basic construction of the considered MHD pumps

The default arrangement of the magnetic circuits of the considered pumps is depicted in Fig. 4a (pumps for molten Na) and Fig. 4b (pump for molten fluoride salt FLiNaK). The default layout of the electric circuits of the considered pumps is shown in Fig. 5. The value of angle $\alpha = 150^\circ$, securing a relatively homogeneous distribution of current density vector (see Fig. 8b), was taken from [7].

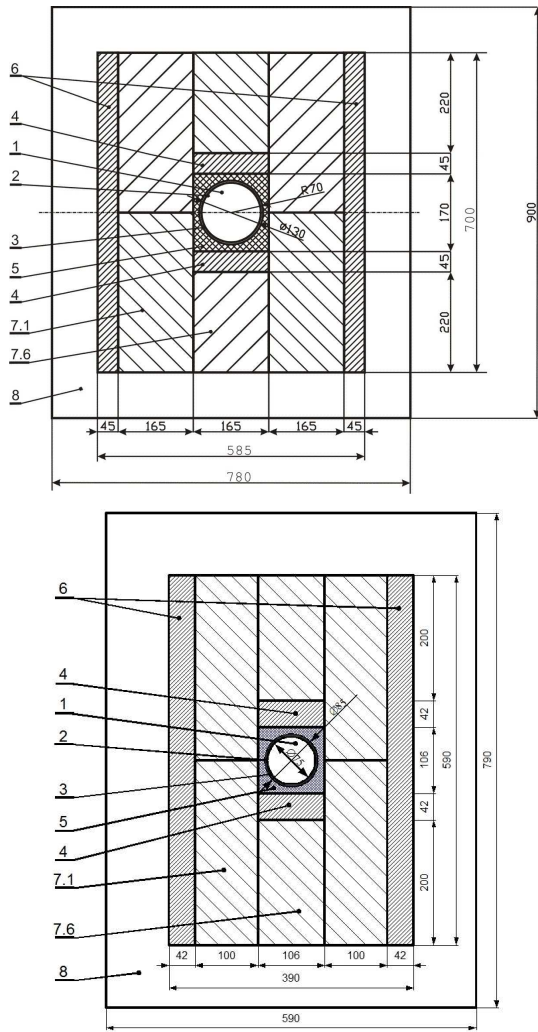


Fig. 4: Magnetic circuit of presented MHD pump: a) pump for molten sodium; b) pump for molten fluoride salt FLiNaK [1-transported liquid; 2- electrodes (austenitic steel ČSN 17 241); 3- tube (molten basalt); 4-ferromagnetic focusators (carbon steel ČSN 12 040); 5-heat insulation of magnets (fiberglass); 6-ferromagnetic bypasses of magnetic flow (carbon steel ČSN 12 040); 7-permanent magnets (NdFeB Magnet, Grade GSN-40, [8]); 8-cooling water]

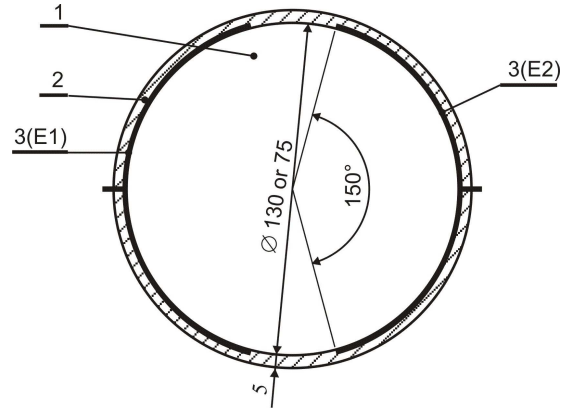


Fig. 5: Electric circuit of presented MHD pumps 1-transported liquid; 2- tube (molten basalt), 3-electrodes

The basic physical parameters of materials used in the presented MHD pumps are listed in Tab. 4.

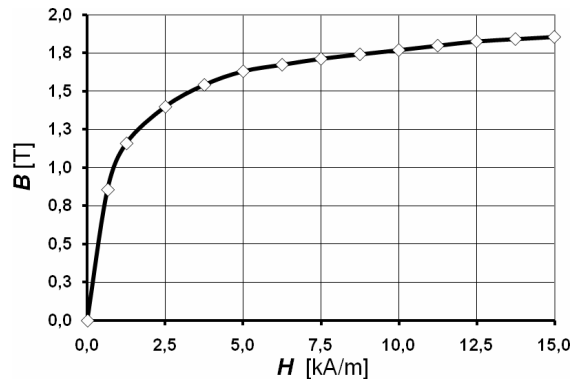


Fig. 6: The $B(H)$ dependence for carbon steel ČSN 12 040 [9]

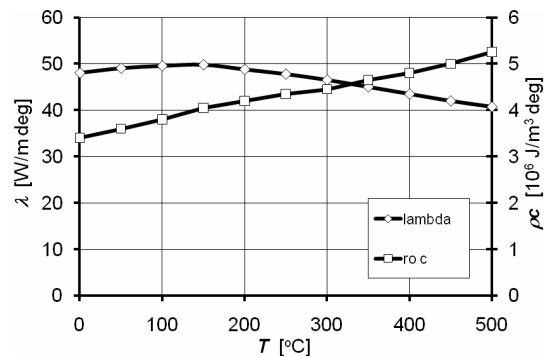


Fig. 7: The $\lambda(T)$ and $\rho c(T)$ dependencies for steel ČSN 12 040 [9]

MATHEMATICAL MODEL

Electric, magnetic and temperature fields in the MHD pump

Provided that the above fields are stationary, it is

possible to describe them with a system of three autonomous partial differential equations:

- Electric and current fields generated by the electrodes

$$\operatorname{div} \operatorname{grad} \varphi = 0, \quad (1)$$

$$\mathbf{J}_e = -\gamma_{el} \operatorname{grad} \varphi. \quad (2)$$

- Magnetic field generated by the system of permanent magnets with the coercive field strength \mathbf{H}_c and remanence \mathbf{B}_r

$$\operatorname{curl} \left(\frac{1}{\mu} \operatorname{curl} \mathbf{A} - \mathbf{H}_c \right) = 0, \quad (3)$$

where

$$\mu = \frac{B_r}{H_c} \quad (4)$$

and

$$\mathbf{B}_m = \operatorname{curl} \mathbf{A}. \quad (5)$$

- Temperature field in the channel

$$\operatorname{div} (\lambda \operatorname{grad} T) = -\frac{J_e^2}{\gamma_{el}}, \quad (6)$$

while

$$\operatorname{div} (\lambda \operatorname{grad} T) = 0 \quad (7)$$

elsewhere.

The physical parameters figuring in these equations for the case of considered MHD pumps are listed in previously mentioned Tab. 4.

Solution of (1), (3), (6) or (7) provides the distribution of potentials φ , \mathbf{A} , and temperature T .

The distribution of vectors \mathbf{J}_e and \mathbf{B}_m ((2) and (5)) in the domain of the channel is determined in the second step.

The vector \mathbf{F}_L of the Lorentz force vector acting on the electrically conductive heat-transfer medium (molted metal or salt) in the working channel is given by the equation

$$\mathbf{F}_L = \int_V (\mathbf{J}_e \times \mathbf{B}_m) dV. \quad (8)$$

Successful operation of the cooling loop with the MHD pump is conditioned by the validity of inequality $|\mathbf{F}_L| \geq |\mathbf{F}_{hd}|$, or $|\mathbf{F}_L| \geq |\mathbf{F}_{hs}| + |\mathbf{F}_{hd}|$, where \mathbf{F}_{hs} is the vector of the hydrostatic force and \mathbf{F}_{hd} is the drag vector due to hydraulic resistances in the cooling loop (see chapter 3.2).

HYDROSTATIC AND HYDRODYNAMIC FORCES IN THE COOLING LOOP

- Hydrostatic force (that should be considered if we work with the open loop – for example during startup of the reactor) is given as

$$F_{hs} = h\rho \frac{\pi D_0^2}{4}, \quad (9)$$

where h is the height of the column of melt, ρ is the specific mass of melt and D_0 stands for the diameter of the loop pipeline.

- Hydrodynamic force – due to the hydrodynamic resistances (this force should be considered if the loop is closed and the working medium is flowing through – for example, during the steady-state operation of the reactor) is given as

$$F_{hd} = \sum_{i=1}^N S_i \nabla p_{d,i}, \quad (10)$$

where S_i is the cross-section of the i th element of the considered loop and $\nabla p_{d,i}$ stands for the corresponding pressure loss.

The pressure loss $\nabla p_{d,i}$ in the i th element of the considered loop can be (see [4], [6]) calculated as

$$\nabla p_{d,i} = \left(\lambda \frac{l}{D} \frac{\rho w^2}{2} \right)_i, \quad (11)$$

where ρ is the specific mass of the transferred melt, w denotes its velocity, and λ is the coefficient of the hydrodynamic resistance in the i th element, whose values can be found in suitable references (see for example [4] or [6]). This coefficient usually depends on the Reynolds number $Re_i = (wD/\nu)_i$, where w is the velocity, D is the characteristic dimension of the i th element and symbol ν stands for the kinematic viscosity of melt.

COMPUTER MODEL OF SOLVED PROBLEM

The mathematical model of this problem was solved as a 2D (x, y) problem and later (mainly for evaluation of the influence of the boundary effects) also as a 3D (x, y, z) problem.

2D (x, y) solution

The 2D solution was realized using the FEM-based program *QuickField* (version 5.6 [10]). The aim was to quickly obtain information about the approximate, but sufficiently accurate distributions of magnetic, electric and temperature fields – for particulars see chapter 5. A great attention was paid to monitoring of the convergence of solution – for results valid in three significant digits it was necessary to use meshes with approximately

- 150×10^3 nodes for magnetic field,
- 60×10^3 nodes for electric field,
- 120×10^3 nodes for temperature field.

Some illustrative results follow. Fig. 8a shows a map of force lines of magnetic field in the system, while Fig. 8b depicts the distribution of equipotentials of electric field in the channel. Fig. 8c depicts the

steady-state temperature field produced by the transported working substance. All the results shown in the above figures are valid for sufficiently long MHD pumps, thus ignoring the front effects.

It is clear that 2D results provide sufficiently accurate qualitative information about the suitability of various considered configurations – for example the total Lorentz force F_L strongly depends on the homogeneity of the electric and magnetic fields or, more accurately, of the corresponding electric and magnetic flux densities. The more detailed presentation and discussion of the obtained results can be found in chapter 5.

3D (x, y, z) solution

The 3D solution was realized using the FEM-based program *COMSOL* (version 3.5 [11]). The aim was to get information about the influence of the boundary effects (in our case the final length of MHD is $l_{ef} = 0.3$ m) and, subsequently, about the accuracy of all 2D calculations, carried out without considering these effects (see Fig. 9c). The problem was solved as a coupled task using modules Magnetostatics and Conductive Media DC of the *COMSOL* program. Processing of this 3D problem requires some limitations due to computer memory. On the other hand, high attention was paid to the convergence of the results obtained. For the final solution we used about 100000 elements. Figures 9a, 9b and 9c show some results whose discussion follows in chapter 5.3.3. Figure 9c depicts the detail of the front effects, but it is rather qualitative information.

ILLUSTRATIVE EXAMPLE

The aim of the presented example is to show the possibility of cooling a nuclear mini-reactor of type RAPID by an MHD pump, to evaluate the basic technical factors affecting the operation of that pump (in particular, configuration of the magnetic and electric circuits), and to evaluate the 2D and 3D models with respect to accuracy of the principal results (such as the total pumping force $w = 1$).

Input parameters of the solved example

The reactor RAPID is considered to be cooled by four cooling loops arranged in accordance with Fig. 3. The loops are closed, filled with the working media. This medium flows through the loop at a velocity w . The basic technical information about the reactor and its cooling loops is given in chapter 2.2 and Table 2. Considered are two types of working substances – molten sodium and molten fluoride salt FLiNaK (LiF 45.3 – NaF 3.2 – KF 41.5 [mol %]). The physical parameters of these substances are listed in Table 1. Chapter 2.2 describes the way of calculation of the hydrodynamic losses in the loops. Their specific values for the selected flow rate $w = 1$ m/s and both

considered types of fluids are listed in Table 3. The basic information about the magnetic and electric circuit of this MHD pump is given in paragraph 2.3, in the corresponding figures, and in Table 4.

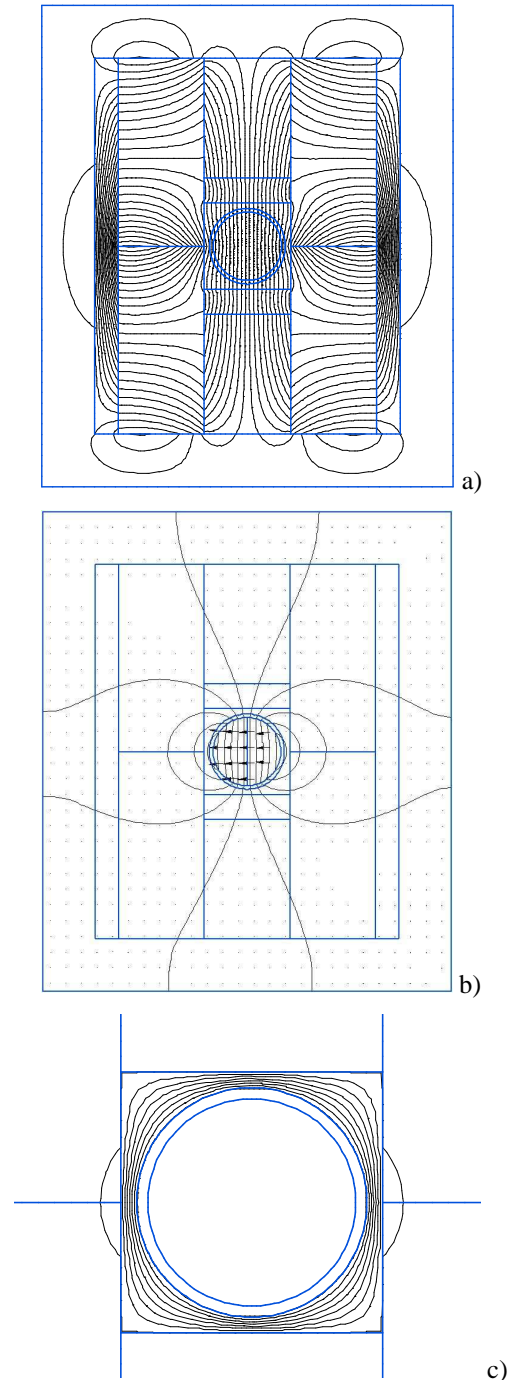


Fig. 8: Illustrative maps of 2D fields in the considered MHD pump (cooling medium is molten sodium, $l_e = 0.3$ m), solved by code *QUICK FIELD* [6]:
a) magnetic field generated by permanent magnets NdFeB Magnet, Grade GSN 40, [8];
b) electric field for $J_{a,x} = 1.303 \times 10^5$ A/m²;
c) temperature field, $T_{\max} \approx T_{\text{work,Na}} = 455$ °C, $\Delta T = 60$ °C and $T_{\min} \approx T_{\text{H}_2\text{O}} = 20$ °C.
(Significance of all symbol is explained in par. 5)

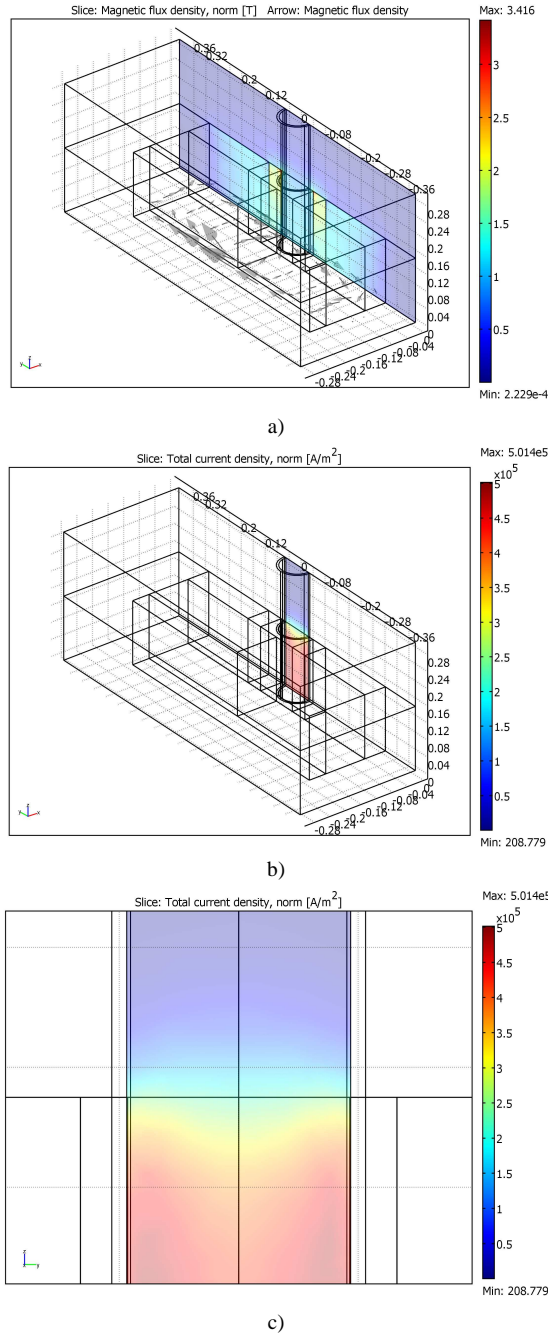


Fig. 9: Illustrative maps of 3D fields in the investigated MHD pump (working medium – molten salt, $l_e = 0.3$ m) obtained from program *COMSOL* [7]:
a) magnetic field (permanent magnets NdFeB Magnet, Grade GSN 40, [8]);
b) electric field, $J_{a,x} = 3.541 \times 10^5$ A/m²;
c) detail of electric field in the area of the top front of the pump;
(For the significance of the symbols see chapter 5)

The possibilities of employment of these MHD pumps in the RAPID reactor

This possibility was checked by calculations carried out for both mentioned fluids (the length of the pump being 0.3 m) and for the best arrangement of pumps – layout 4 – see paragraph 5.3 and Table 5.

The parameters of the pumps calculated for the arrangement 4 and for both types of fluid (molten sodium and molten fluoride salt) with the coefficient of safety $\kappa_b = \frac{F_L}{F_{hd}} = 1.5$ are listed in Table 6.

For calculation of the parameters listed in Table 6 we used the relationship

$$J_{a,x} = \frac{F_{hd} \kappa_b}{B_{a,y} \frac{\pi D_0^2}{4} l_e}, \quad (12)$$

where F_{hd} is the hydrodynamic power loss in the cooling loop, $B_{a,y}$ is the y -component of magnetic flux density, κ_b is the coefficient of safety, D_0 is the diameter of the working channel, and l_e is the length of the working channel.

Formula (12), that can easily be derived from (8), serves for determining the value $J_{a,x}$ (average component of field current density in the x -direction). The value of F_{hd} can be determined from the hydrodynamic conditions in the cooling loop – see paragraph 3.2 and Table 3. The values of $B_{a,y}$ were determined from the stationary magnetic field – see paragraphs 3.1, 4.1, and Table 5.

From the value of $J_{a,x}$ we can determine the required current that is to be applied to the electrodes of the MHD pump. Its value can be found using the inverse solution of electric field (see chapter 3.1, equations (1) and (2)). Here it is necessary to find the boundary condition of the second kind on the electrodes **E1** and **E2** (see Fig. 5), such that we reach the required current density. This can be realized iteratively using the *Regula Falsi* method (see, e.g., [12]).

We can make, therefore, a partial conclusion: From the values listed in Table 6 it is apparent that the desired parameters of the pumps for molten sodium and also molten fluoride salt FLiNaK are in this case completely real and easily realizable at every power station.

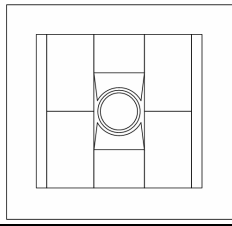
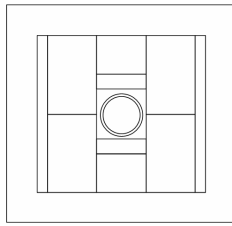
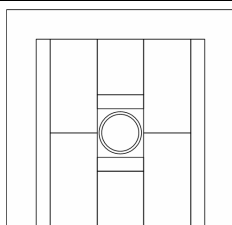
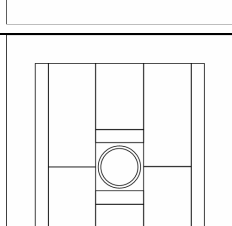
Technical factors affecting the operation of the considered MHD pumps

These basic technical factors are:

The magnetic circuit of the pump

The investigated magnetic circuits of the pump are described and quantitatively evaluated in Table 5. Hence, it is apparent that from the viewpoints of the size and homogeneity of the magnetic flux density in the working area of the MHD pumps are advantageous mainly flat ferromagnetic focusators homogenizing the magnetic field in the working area of the considered magnetic circuit, sufficiently large ferromagnetic bypasses ($b_b = 0.045$ m) and long, correctly oriented permanent magnets ($l_m = 0.65$ m, $b_m = 0.165$ m).

Tab. 5: Evaluation of the initial arrangements of the system of permanent magnets of the MHD pump for pumping molten Na (Fig. 4a)

arrangement		selected parameters
1		circular focusator total height of the magnets: $l_m = 0.52$ m side magnets: $b_m = 0.165$ m Fe bypass: $b_b = 0.035$ m $B_{y,a} = -1.1339$ T
2		direct focusator total height of the magnets: $l_m = 0.52$ m side magnets: $b_m = 0.165$ m Fe bypass: $b_b = 0.035$ m $B_{y,a} = -1.1438$ T
3		direct focusator total height of the magnets: $l_m = 0.65$ m side magnets: $b_m = 0.165$ m Fe bypass: $b_b = 0.045$ m $B_{y,a} = -1.3017$ T
4		direct focusator total height of the magnets: $l_m = 0.715$ m side magnets: $b_m = 0.165$ m Fe bypass: $b_b = 0.045$ m $B_{y,a} = -1.3492$ T

Tab. 6: Calculated parameters of the pumps 4 (see Tab. 5) for both types of working media

parameter	unit	coolant		remark	
		Na	fluoride salt		
hydrodynamic losses ⁽¹⁾ in the loop	Δp_{hd}	[Pa]	527.7	714.0	see Tab. 2
hydrodynamic force in the loop	F_{hd}	[N]	7.001	3.154	
required force ⁽²⁾ in the loop	F_L	[N]	10.50	4.731	
average value of magnetic flux density	$B_{a,y}$	[T]	1.349	1.533	see Tab. 5
corresponding current density ⁽³⁾	$J_{a,x}$	[A/m ²]	1957	2322	
corresponding current passing through electrodes E1, E2	I_e	[A]	88.06	52.38	
resistance of coolant between the electrodes E1, E2	R_e	[Ω]	4.47×10^{-7}	4.240×10^{-3}	
ohmic losses due to the above resistance	$P_e = R_e I_e^2$	[W]	3.46×10^{-3}	11.63	

⁽¹⁾ for more details see Tab. 3

⁽²⁾ generated by the pump with coefficient of safety $\kappa_b = \frac{F_L}{F_{hd}} = 1.5$

⁽³⁾ calculated from (11), for more details see Tab. 3

The specific arrangement of such a magnetic circuit (arrangement 4 according to Tab. 5) is depicted in Fig. 4. This arrangement provides (using magnets NdFeB Magnet, Grade GSN-40, see [8], physical parameters listed in Table 4) in the working area of the MHD pump of length $l_e = 0.3$ m the following values of magnetic flux density:

- $B_{a,y} = 1.349$ T (the working channel with diameter $D_0 = 130$ mm \approx molten sodium)
- $B_{a,y} = 1.533$ T (the working channel with diameter $D_0 = 75$ mm \approx molten fluoride salt)

We can make another partial conclusion: The magnetic flux density in the working channel of the pump can easily be affected by the size (the length l_m) of the used magnets. The length of the pump is not important because one can always “pile” appropriately high bar of magnets.

CONCLUSION

The results calculated in the paper show that in nuclear minireactors of the type RAPID and similar it is possible to employ the MHD pumps for pumping selected cooling media (particularly molten sodium or fluoride salts).

The results obtained from both 2D and 3D solution almost coincide. That is why all informative computations may be carried out as 2D ones, and only the final computation should be realized in 3D.

REFERENCES

- [1] Andrejev P.A., Kanjev A.A., Fedorovič E.D.: Židkomětaleskie těplonositeli jaděrných reaktorov. SudPromGIZ, L. 1959.
- [2] Cowling T.G.: Magnetohydrodynamics. Interscience Publishers Inc., NY 1957.
- [3] Status of Small Reactor Designs without On-Site Refueling. IAEA (International Atomic Energy Agency), Vienna, Aus, 2007, Annex. XVII, Reactor RAPID, pp. 469–489
- [4] Gerbeau, J. B., Le Bris, C., Lelievre, T.: Mathematical Methods for the Magnetohydrodynamics of Liquid Metals. OXFORD University Press, Oxford, GB, 2006.
- [5] Idelchik I.E.: Handbook of Hydraulic Resistance. Begell House, Inc (USA), 1996.
- [6] Cengel Y. A., Turner R.H.: Fundamentals of Thermal-Fluid Sciences. McGraw Hill, NY (USA), 2000.
- [7] Doležel, I., Donátová, M., Karban, P., Ulrych, B.: Pumps of Molten Metal Based on Magnetohydrodynamic Principle for Cooling High-Temperature Nuclear Reactors. Przegląd Elektrotechniczny (Electrical Review), Vol 2009, No 4, pp. 13–16.
- [8] www.goudsmitmagnets.com
- [9] Company Standard ŠKODA 00 6004.
- [10] www.quickfield.com
- [11] COMSOL Multiphysics version 3.5. <http://www.comsol.com>
- [12] Ralston A.: A First Course in Numerical Analysis. McGraw - Hill Book Co., NY 1973.